

Research Article

Investigation of the Physicochemical and Physicomechanical Properties of a Novel Intravaginal Bioadhesive Polymeric Device in the Pig Model

Valence M. K. Ndesendo,¹ Viness Pillay,^{1,6} Yahya E. Choonara,¹ Lisa C. du Toit,¹ Eckhart Buchmann,² Leith C. R. Meyer,³ Riaz A. Khan,⁴ and Uwe Rosin⁵

Received 19 November 2009; accepted 16 April 2010; published online 6 May 2010

Abstract. The purpose of this study was to develop and evaluate the bioadhesivity, *in vitro* drug release, and permeation of an intravaginal bioadhesive polymeric device (IBPD) loaded with 3'-azido-3'-deoxythymidine (AZT) and polystyrene sulfonate (PSS). Modified polyamide 6,10, poly(lactic-coglycolic acid), polyacrylic acid, polyvinyl alcohol, and ethylcellulose were blended with model drugs AZT and PSS as well as radio-opaque barium sulfate (BaSO₄) and then compressed into caplet devices on a tableting press. One set of devices was coated with 2% *w/v* pentaerythritol polyacrylic acid (APE-PAA) while another remained uncoated. Thermal analysis was performed on the constituent polymers as well as the IBPD. The changes in micro-environmental pH within the simulated human vaginal fluid due to the presence of the IBPD were assessed over a period of 30 days. Textural profile analysis indicated that the bioadhesivity of the APE-PAA-coated devices (3.699±0.464 N; 0.0098±0.0004 J) was higher than that of the uncoated devices (1.198±0.150 N; 0.0019±0.0001 J). In addition, BaSO₄-facilitated X-ray imaging revealed that the IBPD adhered to pig vaginal tissue over the experimental period of 30 days. Controlled drug release kinetics was obtained over 72 days. During a 24-h permeation study, an increase in drug flux for both AZT (0.84 mg cm⁻² h⁻¹) and PSS (0.72 mg cm⁻² h⁻¹) was realized up to 12 h and thereafter a steady-state was achieved. The diffusion and dissolution dynamics were mechanistically deduced based on a chemometric and molecular structure modeling approach. Overall, results suggested that the IBPD may be sufficiently bioadhesive with desirable physicochemical and physicomechanical stability for use as a prolonged intravaginal drug delivery device.

KEY WORDS: bioadhesivity; controlled release; intravaginal drug delivery; microbicidal polymeric device; physicochemical and physicomechanical characterization.

INTRODUCTION

The vagina remains a relatively unexplored route of drug delivery in humans despite the potential to be used as a non-invasive route of drug administration (1). In addition, the vaginal route offers numerous advantages as a localized site for drug delivery due to convenient access, prolonged retention of formulations, an extensive region for drug permeation, high vascularization, a relatively low enzymatic activity, the avoidance of gastrointestinal and/or hepatic first-pass metabolism, and the possibility of self-administration of

single-dose drug delivery systems that may suffice in releasing drugs over a period of weeks or months and simultaneously provide optimum drug pharmacokinetic profiles (2–4). Thus, intravaginal drug delivery has exploitable advantages compared to other routes of administration in the area of bioavailability and controlled drug delivery (5–16). A contributing factor to the exploitable advantages conferred by the vaginal route of drug administration is the fact that the adult vaginal cavity has an extensive surface area (100–150 cm²) that is adequately accessible for self-administration purposes (17). Furthermore, the vaginal route provides room for continuous programmed administration of drugs while simultaneously prevents the superfluous peaking of plasma levels that is often seen with the use of oral drug delivery systems administered as discrete discontinuous doses (17,18). However, the localization and prolongation of a drug delivery system at a specific target site with the maintenance of direct contact with the vaginal epithelium in order to increase the drug concentration gradient is still a challenge (2). This may be overcome by the use of bioadhesive drug delivery devices. The adhesion of a delivery system to mucosal membranes may lead to an increase in drug concentration at the site of action. This may allow greater quantities of drug to be available for absorption to affect the desired therapeutic

¹ Department of Pharmacy and Pharmacology, University of the Witwatersrand, 7 York Road, Parktown, 2193, Johannesburg, South Africa.

² Department of Gynecology and Obstetrics, Chris Hani Baragwanath Hospital, Bertsham, 2013 Johannesburg, South Africa.

³ Central Animal Services, University of the Witwatersrand, 7 York Road, Parktown, 2193 Johannesburg, South Africa.

⁴ Department of Industrial Chemistry, Integral University, Lucknow, 226026 India.

⁵ Research and Development Unit, PharmaNatura (Pty) Ltd., Sandton, 2012 South Africa.

⁶ To whom correspondence should be addressed. (e-mail: viness.pillay@wits.ac.za)

outcome. Thus, successful development of an intravaginal drug delivery system should consider characteristics of the formulation design, the therapeutic agent, and vaginal physiology (3,12,19).

Given the devastating effects of the HIV/AIDS epidemic and enduring challenges in developing an effective HIV vaccine, coupled with the disempowerment of some women that renders them unable to refuse unsafe sexual practices in certain communities (19), it is evident that there is an urgent need for developing simple, inexpensive, and acceptable approaches for the prevention of HIV/AIDS and STIs in addition to the latex condom. While numerous drugs and drug delivery systems are being developed, there is still a dire need for new and improved localized drug delivery formulations that will be accepted by the majority of women (19,20). One approach that has been explored in this study is the development of a bioadhesive caplet-shaped dual microbical delivery device for intravaginal insertion prior to or immediately after intercourse for prevention HIV/STIs transmission. The device is formulated from a precisely selected biodegradable and biocompatible polymer blend and is termed an intravaginal bioadhesive polymeric device (IBPD). The device may be suitable for intravaginal drug delivery that provides controlled drug release kinetics. The thermodynamic behavior of polymers is known to have a significant impact on the physicochemical properties and therefore their final performance (21,22). Therefore, accurate thermal analysis of polymer blends employing temperature-modulated differential scanning calorimetry (TMDSC) is critical for formulation design (23). TMDSC provides a clearer interpretation of thermal transitions on analyzed samples due to the improved sensitivity and resolution, coupled with the ability to separate reversible glass transitions that have diminutive transitions in heat capacity from overlapping non-reversible relaxation endotherms. TMDSC is also used to reveal thermal transitions at sub-zero temperatures that cannot be detected by conventional DSC due to poor equilibrium of the heat flow baseline below 0°C (24).

The permeation of most of the drugs across biological tissues has been investigated and presumed to occur through two mechanisms, namely the paracellular (between adjacent epithelial cells) and transcellular (across epithelial cells) routes by means of either passive diffusion, carrier-mediated transport, or endocytosis (25–27). Generally, drug diffusion rates correlate with partition coefficients and are inversely proportional to the molecular mass of the drug (3). For the successful development of an intravaginal drug delivery system, the greatest challenge lies in designing a system that is retainable and can provide a high drug concentration in the vagina over a prolonged period of time (2).

Therefore the aim of the present study was to design and develop a novel intravaginal bioadhesive polymeric device to prevent sexual transmission of HIV and other STIs. The model drugs/bioactives selected for loading into the IBPD were AZT and polystyrene sulfonate (PSS). The device would provide controlled drug release over an experimental period of at least 1 month when inserted into the posterior fornix of the vaginal cavity. The anterior and posterior vaginal fornices are anatomical recesses that exist due to the projection of the cervix into the vagina. The posterior fornix is the deeper of the two fornices and is most isolated from

external interference as a result of menses, coitus, or the application of other therapeutic modalities that may be inserted. The posterior fornix is also located away from the path of menstrual flow, since it lies behind and above the cervix. Therefore, menstrual cycles and shear stress from promiscuous sexual activity will not affect the ability of the IBPD to maintain its adherence in the posterior fornix of the vagina. Thus, the posterior fornix location was purposely chosen so as to avoid any interference to the formulation during menses and sexual intercourse. Since the device was intended to provide prolonged intravaginal drug delivery and subsequent prophylaxis against HIV and STIs a select group of polymers were chosen. These polymers included combinations of biomaterials that were able to impart their inherent properties to constitute the optimal intravaginal formulation for the intended application. Five polymers were employed namely modified polyamide 6,10 (m PA 6,10), poly(lactide-co-glycolic acid) (PLGA), polyacrylic acid (PAA), polyvinyl alcohol (PVA), and ethylcellulose (EC) for preparing the AZT and PSS-loaded IBPD. It was imperative to employ the selected five polymers since each possessed distinct functions based on their intrinsic properties. Modified polyamide 6,10 has a high modulus, thermoplasticity, matrix resilience, abrasion resistance, and chemical inertness. It was thus employed to control drug release, facilitate permeation of drug, and to intensify the robustness of the IBPD. Poly(lactic co-glycolic acid) was selected due to its hydrophobicity and ability to degrade into two acidic units namely lactic and glycolic acid. The presence of these acidic units will produce an acidic pH environment within the vagina upon degradation and thus maintain the normal vaginal ecology by favoring the growth of *Lactobacilli*-containing microflora that prevents bacterial vaginosis. Furthermore, due to its hydrophobic nature it may aid in controlling drug release from the IBPD. Ethylcellulose is also a hydrophobic and easily compressible polymer. It was therefore selected for formulation of the IBPD. Polyvinyl alcohol, a hydrophilic, compressible, and mildly bioadhesive polymer was included to foster bioadhesivity in conjunction with polyacrylic acid to induce surface energy interactions that favor spreading onto the vaginal mucus for maximal intravaginal tissue retention of the drug.

PSS played a dual role as a matrix polymer and bioactive (28,29). PSS acts as a topical broad spectrum antimicrobial agent that can prevent the adherence of the Herpes Simplex Virus at low concentrations and inactivates the virus at higher concentrations (28–34). PAA was used as both polymer matrix constituent as well as a coating agent for the purpose of achieving extended bioadhesivity within the posterior fornix of the vagina (35,36). An X-ray imaging approach employing radiopaque barium sulfate ($BaSO_4$) was developed for detecting and determining the sequential biodegradation pattern of the IBPD device in the vagina of the Large White pig as the most suitable animal model for *in vivo* evaluation of the device. $BaSO_4$ was employed as a dual-function formulation excipient in that it imparted matrix stabilization at higher concentrations in addition to its radiopaque properties that facilitated X-ray imaging of the device in the pig vagina. The Large White pig model was selected for this study due to the similarity in the human and pig vagina, particularly the genital tract physiology and histology (37–39). In addition, $BaSO_4$, which is biocompatible, exhibited desir-

able properties of stabilizing the polymeric matrix integrity (40). The acidic environment in the vagina may be influenced by the changes in pH and ionic concentrations as a result of PLGA degradation into lactic and glycolic acid through cleavage by enzymatic or non-enzymatic hydrolysis (41–43). Thus, since PLGA was one of the polymers selected for formulating the IBPD, it was important to determine the changes in micro-environmental pH of the simulated human vaginal fluid (SHVF) when exposed to the degrading constituents of the IBPD. In addition, since chemometric and molecular modeling approaches can precisely explicate various interactive mechanisms of drug release and diffusion dynamics that occur from a drug delivery system, it was employed in this study to elucidate these mechanisms at a molecular level.

MATERIALS AND METHODS

Materials

Modified polyamide 6,10 was synthesized using a previous method developed by Kolawole and co-workers (44). Poly(lactide-co-glycolide) (Resomer® RG504) was purchased from Boehringer Ingelheim (Ingelheim, Germany). The other commercially available polymers used were allyl pentaerythritol polyacrylic acid (APE-PAA; Carbopol® 974, Noveon Inc., Cleveland, OH, USA), polyvinyl alcohol (Merck-Schuchardt, Hohenbrunn, Germany), and ethylcellulose (Ethocel-10®, Sigma-Aldrich Chemie, Steinheim, Germany). The two model drugs were 3'-azido-3'-deoxythymidine (Evershine Ind., Naejar Malad, Mumbai, India), and polystyrene sulfonate (as a sodium salt; Omega (Pty) Ltd., Montreal, Canada). Methylparaben (Merck (Pty) Ltd., Darmstadt, Germany), shellac (Roeper GmbH, Hamburg, Germany), castor oil (Jayant Oils and Derivatives Ltd., Mumbai, India), and calcium hydroxide (Associated Chemical Enterprises (Pty) Ltd., Southdale, South Africa) were used as formulation stabilizers. Barium sulfate (Merck-Schuchardt, Hohenbrunn, Germany), albumin bovine serum (Sigma-Aldrich Chemie, Steinheim, Germany), acetic acid (Holpro Analytic (Pty) Ltd., Johannesburg, South Africa), and glycerol (Associated Chemical Enterprises (Pty) Ltd., Southdale, South Africa) formed part of the simulated human vaginal or seminal fluids. Pentobarbitone, ketamine (Bayer (Pty) Ltd, Wrenchweg, Isando, South Africa), midazolam (Roche Products (Pty) Ltd, Isando, Gauteng, South Africa), and isoflurane (Safe Line Pharmaceuticals (Pty) Ltd, Florida, South Africa) were utilized to facilitate the *in vivo* evaluation of the device. The mobile phase solvents composed of acetonitrile (99.9%) and methanol (99.9%) that were purchased from Romil-SpS™ (Cambridge, UK) including ultra performance liquid chromatography (UPLC) grade water (Milli-Q® A10 System, Millipore®, Molsheim, France). All other reagents used were of analytical grade and were employed as purchased.

Preparation of the Intravaginal Bioadhesive Polymeric Device

An extreme vertices mixture design (EVMD) template was generated employing Minitab® V15 (Minitab® Inc., PA,

USA) statistical software to produce various caplet formulations comprising 11 polymer combinations. Each formulation had an equivalent mass of 800 mg. Formulation response optimization was performed using an inherent D-optimal technique by combining mixture components and processing factors to converge to pre-optimal settings prior to achieving a global optimized solution with the desirable polymeric proportions. Two crosslinked forms of polyacrylic acid were tested interchangeably namely allyl sucrose-crosslinked PAA (AS-PAA) and allyl penta erythritol-crosslinked PAA (APE-PAA). Following the results obtained from EVMD template, biodegradable and biocompatible polymers namely mPA 6,10 (150 mg), PLGA (400 mg), APE-PAA (25 mg), PVA (25 mg), and EC (200 mg; which comprised the most optimal formulation) were blended with model drugs AZT (200 mg) and PSS (200 mg) using a cube blender (Erweka® GmbH, Heusenstamm, Germany). Radiopaque BaSO₄ (500 mg) was then added and the powder blend was compressed at a pressure of 25 tons into two sets of caplet-shaped devices on a Manesty D3B 16 station tableting press equipped with D3B oblong tooling of 5×9×22 mm in dimension (Manesty D3B L249LQ, Liverpool, England). In process validation tests were performed to ensure that the IBPD device had desirable quality attributes in terms of matrix hardness, uniformity in mass, and friability.

Pan-Coating of the Intravaginal Bioadhesive Polymeric Device

A dual coating process using the Thai Coater® (Pharmaceutical and Medical Supply Limited Partnership, Yan-nawa, Bangkok, Thailand) was employed with a protective undercoat comprising shellac and thereafter a mixture of XG and APE-PAA as an overcoat in order to prevent any irritation to the vaginal tissue during device insertion. The addition of APE-PAA was to facilitate bioadhesion of the IBPD to the posterior fornix of the vagina. The process involved firstly undercoating the IBPD with a combination of shellac (4 mg/device), cold-pressed castor oil (3 mg/device), and ethanol (96%). This was followed by an overcoat of XG (2% w/v) and APE-PAA (2% w/v). XG was used for its viscoelastic non-collapsible swellability (45–47) in order to facilitate bioadhesion of the IBPD in conjunction with APE-PAA that is also bioadhesive. The processing conditions utilized for effective coating of the IBPDs were as follows: (1) coating temperature ranged from 50–56°C; (2) relative humidity ranged between 23% and 28%; (3) warming up period was 10 min; (4) the pan was rotated at 2–3 rpm; (5) spray rate was 4 g/min; (6) undercoating duration was 30 min; and (7) the over-coating duration was 60 min. A non-coating period of 30 min was allowed after each coating phase to effect a reduction in pan temperature and avoid sticking or fracture of the undercoat or overcoat seal. The increase in weight after coating the IBPD was determined using a digital balance (Mettler, Model AE 240, Griefensee, Switzerland) while the increase in thickness was determined using a digital vernier caliper (Taizhou Hangyu Tools Gauge and Blades Co., Ltd, Wenqiao, Zhejiang, China) with a sensitivity of 0.01 mm.

In Vitro Drug Release from the Coated and Uncoated Intravaginal Bioadhesive Polymeric Device

Analysis of the Effect of Device Coating on Drug Release

To assess the effect of coating on drug release, analysis was conducted on IBPDs (coated and uncoated) containing AZT as a representative drug model due to its hydrophilicity. An IBPD was immersed in a 100 mL (48,49) SHVF (pH 4.5; 37°C (50); Table I) using a sealable glass vessel (150 mL) and placed in an orbital shaking incubator (LM-530-2, MRC Laboratory Instruments Ltd., Hahistadrut, Holon, Israel) maintained at 20 rpm and a temperature of 37°C. For the determination of AZT concentration, 3 mL samples were withdrawn at predetermined time intervals over a period of 30 days and subjected to ultra performance liquid chromatography analysis. An equivalent volume of drug-free SHVF was replaced into the release medium to maintain sink conditions. The analysis was conducted in triplicate. A correction factor was appropriately applied in all cases where dilution of samples was required.

Analysis of Drug Release from the Coated Devices Containing AZT and PSS Separately and in Combination

For the analysis of the drug release from the coated devices containing AZT and PSS separately and in combination, the same procedure as described earlier was employed, the only difference being that in this case samples for analysis were withdrawn over a period of 11 weeks.

Chromatographic Conditions for the Analysis of AZT and PSS Concentration

Quantitative analysis was performed using a Waters® Acquity ultra performance liquid chromatographic system (Waters Corp., Milford, MA, USA), equipped with a photodiode array detector and interchangeable columns, namely, a UPLC® BEH phenyl column (1.7 µm; 2.1×50 mm) for AZT separation, and a UPLC® BEH C₁₈ column (1.7 µm; 2.1×

100 mm) for PSS separation. The binary mobile phases were composed of water/acetonitrile (60:40 *v/v*) and methanol/water (50:50 *v/v*) for AZT and PSS, respectively. All solutions were filtered using a 0.22-µm membrane filter (Millipore Corp., Bedford, Massachusetts, USA) prior to injection onto the UPLC column. For AZT, a gradient method was used at a column temperature of 25°C, injection volume 2 µL, flow rate 0.5 mL/min, and UV detection wavelength of 267 nm. The water/acetonitrile quantities varied from 60/40% at 0.0 min, 5/95% (from 1.0–2.6 min), and finally 60/40% (from 3.5–3.6 min). An isocratic assay method was used for PSS separation employing methanol/water (50:50 *v/v*) as the mobile phase, a flow rate of 0.2 mL/min, a column temperature of 25°C, an injection volume of 1.7 µL and a UV detection wavelength of 244 nm.

Preparation of Calibration Standards

The internal standard employed for both model drugs was methylparaben (MP). Standard solutions of AZT, PSS, and MP (internal standard) were separately prepared by mixing specific quantities in water/acetonitrile (60:40 *v/v*) for AZT and methanol/water (50:50 *v/v*) for PSS to yield a concentration of 0.1 mg/mL in each case. The standard solutions employed in preparing the calibration curve of the test drug and internal standard were obtained by further serial dilutions with a final concentration range of 25–10,000 ng/mL. The internal standard solution was prepared at a concentration of 5,000 ng/mL and was added to all samples prepared for UPLC analysis. Calibration curves were developed using blank SHVF (pH 4.5) and computed as a ratio of the area under the curve (AUC) of AZT and PSS chromatographic peaks to that of the internal standard MP against the corresponding standard concentrations of AZT and PSS.

Solid-Phase Extraction Employed for Drug Quantification from SHVF Samples

This was carried out by using single-use Water Oasis® HLB 3 mL (60 mg) extraction cartridge (Waters Corporation,

Table I. Constituents Used to Prepare the Simulated Human Seminal, Vagina and Plasma Fluids

SHVF (pH 4.5)		SHSF (pH 7.0)		SHPF (pH 7.4)	
Component	QTY(g/L)	Component	QTY(g/L)	Component	QTY(g/L)
NaCl	3.510	NaH ₂ PO ₄ ·H ₂ O	16.974	KH ₂ PO ₄	0.144
KOH	1.400	Na ₂ HPO ₄	17.466	Na ₂ HPO ₄	0.795
Ca(OH) ₂	0.222	Na ₃ C ₃ H ₅ O(CO ₂) ₃	8.130	NaCl	9.000
BSA	0.018	KCl	0.908		
Lactic acid	2.000	KOH	0.881		
Acetic acid	1.000	CaCl ₂	1.010		
Glycerol	0.160	MgCl ₂	0.920		
Urea	0.400	ZnCl ₂	0.344		
Glucose	5.000	Glucose	1.020		
		Fructose	2.720		
		Urea	0.450		
		Lactic acid	0.620		
		BSA	50.400		

SHVF simulated human vaginal fluid according to Owen *et al.* (50); SHSF simulated human plasma fluid according to Giannola *et al.* (51); SHPF simulated human seminal fluid according to Owen and Katz (52); QTY(g/L) quantity (g/L) BSA bovine serum albumin

Milford, Massachusetts, USA) adapting a method developed by Notari and co-workers (53). The solid-phase extraction cartridge was conditioned with 1 mL methanol followed by 1 mL water Milli-Q. For AZT sample preparation, 1 mL of sample was mixed with 1 mL of acetonitrile vortexed for 1 min and centrifuged (Nison Instrument (Shanghai) Limited, Shanghai, China) at 13,000 rpm for 6 min at 24°C. Six hundred fifty microliters of the supernatant was diluted by adding water Milli-Q (1 mL) and loaded in the cartridge. Thereafter, the cartridges were washed with 1 mL of 5% *v/v* methanol in water Milli-Q. Analytes were eluted by washing cartridges with 550 μL 0.01 M KH_2PO_4 followed by 2 mL methanol. The eluate was evaporated to dryness in a slow stream of high-purity nitrogen gas (Afrox, Germiston, Gauteng, South Africa). The extracted sample was re-constituted with 100 μL absolute methanol, mixed with 400 μL of MP, and then filtered into the injection vials using 0.22- μm syringe-driven filter units (Millipore Corporation, Bedford, Massachusetts, USA) for UPLC analysis. The same procedure was followed for PSS samples; however, methanol was used as the mobile phase.

Ex Vivo Drug Permeation Studies Through Pig Vaginal Tissue from the Intravaginal Bioadhesive Polymeric Device

The permeation studies to assess the extent of drug permeation across pig vaginal tissue were performed using a Franz diffusion cell apparatus (PermeGear Inc. Bethlehem, PA, USA) equipped with a 12-mL receptor compartment, clamp, and stirrer-bar. Freshly excised pig vaginal tissue obtained from the euthanized Large White pig described above was placed between the donor and receptor compartments of the FDC apparatus. Ten milliliters simulated plasma (pH 7.4; 37°C (51); Table I) was used in the receptor compartment and continuously agitated. IBPD devices containing AZT and PSS were dissolved in 50 mL SHVF (pH 4.5; 37°C; Table I) and assessed for the permeation of the drug across the pig vaginal tissue (thickness = 1.5 ± 0.06 mm; permeation area = 2.0 ± 0.01 cm^2) and into the simulated plasma in the receptor compartment. Samples (2 mL) were withdrawn from the receptor compartment, at predetermined intervals over a period of 24 h, and subjected to quantitative drug analysis using UPLC. An equivalent volume of drug-free simulated plasma was replaced into the receptor compartment to maintain sink conditions throughout the permeation study. The analyses were conducted in triplicate. A correction factor was appropriately applied in all cases where dilution of samples was required. The extent of permeation of AZT and PSS across the pig vaginal tissue was determined in terms of drug flux. The flux ($\text{mg cm}^{-2} \text{h}^{-1}$) of drug across the vaginal tissue was calculated at steady-state per unit area by linear regression analysis of the permeation data using the equation below.

$$J_s = \frac{Q_r}{A \times t} \quad (3)$$

where, J_s is the drug flux ($\text{mg cm}^{-2} \text{h}^{-1}$), Q_r (mg) is the quantity of AZT or PSS that diffused through the pig vaginal tissue into the receptor compartment, A (cm^2) is the effective cross-sectional area available for drug permeation, and t (h) is the time of drug exposure to the vaginal tissue.

UPLC Analysis of AZT and PSS from Simulated Human Plasma Samples

The chromatographic conditions for the analysis of AZT and PSS concentration in the simulated human plasma fluid (SHPF) were the same as described. Preparation of standard solutions and calibration curves was conducted in the same way as described, the only difference being that calibration curves were developed using blank SHPF (pH 4.5; Table I) instead of SHVF. The solid-phase extraction procedure employed in the extraction of the drugs from SHPF samples was the same as described.

Postulated Mechanism of Drug Permeation and Dissolution Dynamics from the Intravaginal Bioadhesive Polymeric Device Employing Chemometric and Molecular Modeling

Chemometric and molecular structural modeling was used to deduce the transient mechanisms of diffusion and dissolution, chemical interactions, and inter-polymeric interfacing during the dissolution of the IBPD device and the permeation of AZT and PSS across the vaginal tissue. This approach allowed us to make predictive findings based on the chemical and physical interactions underlying the dissolution of the IBPD and the diffusion of AZT/PSS from the IBPD (contained in the SHVF) and finally the permeation of these drugs to SHPF across the pig vaginal tissue. In addition, semi-empirical quantum mechanics were employed to generate molecular interactions and computational energy paradigms of the IBPD components based on inherent interfacial phenomena underlying the mechanisms of dissolution and diffusion as provided by the inter-polymeric blended IBPD. Models and graphics supported on the step-wise molecular IBPD-simulated fluids and IBPD-tissue interactions, polymeric interconversion, dissolution and diffusion as envisioned by the molecular behavior, and stability of the gelled IBPD network were generated on ACD/I-Lab, V5.11 (Add-on) software (Advanced Chemistry Development Inc., Toronto, Canada, 2000).

Influence of the Intravaginal Bioadhesive Polymeric Device on the Micro-environmental pH of the Vagina

The changes in micro-environmental pH within SHVF due to the presence of the IBPD were assessed by incubation of 3 mL SHVF (Table I; containing the IBPD) in a Multi Purpose Titrator (MPT-2) equipped with a rapid response, liquid-filled glass pH micro-electrode supported on a vertical puller (Malvern Instruments Ltd., Worcestershire, UK). The changes in pH were evaluated from a pH-time profile over 30 days. The electrode calibration standards were adjusted to cover the buffer range from pH 3.5–5.5 with a linear Nernstian response maintained.

Thermal Analysis of the Composite Intravaginal Bioadhesive Polymeric Device

Thermal analysis was performed on the constituent polymers ($_m\text{PA}$ 6,10, PLGA, PAA, PVA, and EC) as well as the unhydrated and hydrated physical mixtures of the

polymers and the IBPD using TMDSC (Mettler Toledo, DSC1, STAR^o System, Schwerzenback, Switzerland) in order to assess the individual thermal behavioral transitions. The thermal events were explicated in terms of the glass transition (T_g) measured as the reversible heat flow (ΔH) due to changes in the magnitude of the C_p -complex values (ΔC_p), melting (T_m), and crystallization (T_c) temperature peaks which are consequences of irreversible and reversible ΔH values corresponding to the total heat flow. The temperature calibration was accomplished with the melting transition of indium. The transitions of the individual polymers and their physical mixtures were compared with the transition of the composite IBPD matrix. Samples were weighed (5 mg) on perforated 40 μ L aluminum pans, crimped, and then ramped from -35°C to 230°C on TMDSC under a nitrogen atmosphere (Afrox, Germiston, Gauteng, South Africa) in order to diminish oxidation at a rate of $1^\circ\text{C}/\text{min}$. The instrument parameters and settings employed are listed in Table II.

Ex Vivo Bioadhesivity Testing of the Intravaginal Bioadhesive Polymeric Device

Excision of Vaginal Tissue from the Pig Model

A Large White female pig (84 kg) was euthanized with 40 mL of sodium pentobarbitone (200 mg/mL) administered intravenously. The pelvic canal of the pig was opened by dissecting through the symphysis pubis and then exposing the intra-abdominal vaginal tract (the vestibulum). The external vaginal tract was carefully dissected from the surrounding tissues before removing the vaginal tissue. An incision was made through the vaginal canal to expose the inner lining of the tissue, which was then placed in an airtight specimen jar and immediately subjected to bioadhesivity testing.

Textural Profiling Analysis to Determine the Bioadhesivity of the Intravaginal Bioadhesive Polymeric Device

Bioadhesivity of the IBPD was determined using a previous textural profile analysis method developed by Ndesendo and co-workers (36). Briefly, the freshly excised pig vaginal tissue was secured on the textural probe and the

IBPD was fixated onto the heated textural platen after exposure to SHVF (pH 4.5, 37°C ; Table I) for 30 min. Testing was then conducted by measuring the maximum force (N) required to detach the vaginal tissue from the fixated device. This was determined by measuring the peak adhesive force (PAF) or the work of adhesion that was computed as the area under the curve of a force–distance textural profile (AUC_{FD}). The conditions under which bioadhesivity testing was undertaken constituted a simulated clinical environment using a modified textural analysis experimental technique. A heated platen ($37\pm 0.5^\circ\text{C}$) was used to maintain simulated vaginal conditions prior to fixating the IBPD and during analysis. In addition, all experimentation was performed using simulated human vaginal fluid (pH 4.5; 37°C) as the bioadhesivity test medium.

In Vivo Bioadhesivity Testing of the Intravaginal Bioadhesive Polymeric Device

Insertion of the Intravaginal Bioadhesive Polymeric Device into the Vagina of the Pig Model

Three Large White pigs each weighing 35 kg were anesthetized with midazolam (0.3 mg/kg I.M.) and ketamine (11 mg/kg I.M.). Two percent isoflurane in 100% oxygen was administered via a face mask to maintain anesthesia. The IBPD was then deeply inserted into the posterior fornix of the vagina of each pig with the aid of an applicator and a speculum.

X-Ray Imaging of the Pig for Detection of the Intravaginal Bioadhesive Polymeric Device

To detect the presence, position, and retention of the IBPD in the pig vagina after insertion, animals were X-rayed (Siemens AG, Medical Engineering Group, Erlangen, Germany) directly after device insertion and thereafter three times weekly for 2 weeks, then twice weekly for a further 2 weeks to confirm the presence of the IBPD in the vagina and to analyze its swellability and bioerosion dynamics.

RESULTS AND DISCUSSION

Preparation of the Intravaginal Polymeric Device

Optimization of the extreme vertices mixture design template resulted in a formulation comprising $m\text{PA}$ 6,10 (150 mg), PLGA (400 mg), APE-PAA (25 mg), PVA (25 mg), and EC (200 mg) (F1, Table III) as the most optimal with desirable polymeric proportions for achieving desirable bioadhesivity and prolonged local delivery of AZT and PSS in the vagina. The optimal formulation obtained from the EVMD template was used for investigating the physicochemical and physicochemical properties of the IBPD throughout this study.

Coating of the Intravaginal Bioadhesive Polymeric Device

Uniformly coated IBPDs were produced. The final mass for the coated caplets was 1278 ± 0.04 mg while the uncoated caplets weighed 1200 ± 0.01 mg. Thus, the increase in weight was $6.5\pm 0.02\%$ w/w for which the thickness of the coat was 0.520 ± 0.005 mm.

Table II. Temperature-Modulated Differential Scanning Calorimetry Settings Employed for Thermal Analysis of the Intravaginal Bioadhesive Polymeric Device

Segment type	Setting
Sine phase ^a	
Start	-35°C
Heating rate	$1^\circ\text{C}/\text{min}$
Amplitude	0.8°C
Period	0.8°C
Loop phase ^b	
To segment	1
Increment	0.8°C
End	230°C
Count	436

^a Sinusoidal oscillations

^b Oscillation period

Table III. Extreme Vertices Mixture Formulation Design Template for Caplet Preparation

F #	mPA 6,10 (mg)	PLGA (mg)	EC (mg)	PVA (mg)	AS-PAA (mg)	APE-PAA (mg)
1	150	400	200	25	25	25
2	200	250	300	25	25	25
3	130	260	250	110	50	50
4	200	100	250	150	100	100
5	175	200	250	50	125	125
6	185	275	240	25	75	75
7	175	250	300	25	50	50
8	175	300	275	25	25	25
9	100	50	100	100	225	225
10	200	50	150	200	200	200
11	105	140	175	130	250	250

AS-PAA allyl sucrose-crosslinked PAA, APE-PAA allyl penta erythritol-crosslinked PAA, F# formulation number

F# Formulation number

mPA 6,10 modified polyamide 6,10

EC ethylcellulose

PVA polyvinyl alcohol

PLGA poly(lactic-co-glycolic acid)

Analysis of Drug Release from the Coated and Uncoated Optimized Intravaginal Bioadhesive Polymeric Device

A UPLC assay method was used for quantifying the concentration of AZT and PSS released from the IBPD. Chromatograms depicting the retention times for MP (internal standard), AZT, and PSS in SHVF are as shown in Fig. 1a and b.

Assessment of the Effect of Coating on Drug Release from the Intravaginal Bioadhesive Polymeric Device

The shellac/polyacrylic-acid-coated IBPD containing only one of the model hydrophilic drugs, AZT, demonstrated extended drug release when compared to the uncoated devices (28 vs. 20 days; Fig. 2). This was due to the shielding effect of the initial shellac undercoat and APE-PAA overcoat applied. Once the APE-PAA coating was hydrated the shellac gradually solubilized in a manner that diffusion channels formed within the coating layer. This facilitated the drug diffusion from the IBPD. Furthermore, shellac (used as an undercoat) shielded the device against the ingress of release medium due to its wax-like properties (54). This may be attributed to its inherent moisture protecting properties, as well as its ability to act as a plasticizer.

Analysis of Drug Release from the Optimized Coated Intravaginal Bioadhesive Polymeric Device Containing AZT and PSS Separately and in Combination

The substantial matrix integrity imparted by the polymers used to formulate the IBPD resulted in the minimization of the rate of matrix disentanglement and consequently prolonged and controlled the release of AZT and PSS from the IBPD. Controlled drug release representing zero-order was realized consistently over 40 days for AZT and 72 days for PSS (Fig. 3). These results can be attributed to the hydrophobic nature and high compressibility of EC, PLGA, and PSS, coupled with the superior matrix resilience of mPA 6,10. The electrolytic nature of BaSO₄ may have also contributed to the prolongation and control of drug release. The PSS-loaded IBPD achieved superior drug release behav-

ior with consistent and controlled release over a period of 72 days (Fig. 3d). For the IBPD loaded with both PSS and AZT, the release of PSS occurred over 56 days compared to 40 days for AZT (Fig. 3b and c). However, this was still diminutive in comparison to the 72 days achieved from the PSS-only loaded IBPD (Fig. 3d). Conversely, the period of AZT release from the IBPD was more prolonged than from the AZT-only loaded IBPD device (i.e., 40 vs. 28 days; Fig. 3a and b). This was clear that the inclusion of PSS had a significant role in controlling the release of AZT from the IBPD due to the hydrophobicity of PSS and electrostatic and/or electrolytic properties (as a sodium salt) arising from its polymeric segmental charge density (55). Studies have shown that charge density of polyelectrolytes such as PSS enhance binding interactions and favors oppositely charged compounds, culminating in the lowering of the rate of desorption and diffusion thereby slowing the drug release rate from the polyelectrolyte compound (55,56). The hydrophobicity of PSS results from the presence of strong electrostatic charges and internal linkages (H- and S-bonds) in the residual un-sulfonated aromatic moieties of the PSS molecule (57,58). In addition, previous studies conducted on polyelectrolytes such as PSS have shown that the higher the osmotic coefficient and radius of gyration, the greater the ability to control the rate of drug release (59–64).

Assessment of Drug Permeation Across the Pig Vaginal Tissue

Since the pharmacokinetic and pharmacodynamic performance of the IBPD in the vaginal cavity is critical for ascertaining that a clinical benefit is realized with this approach, adequate local delivery within the vaginal tissue has been assessed under the permeation kinetic studies to ascertain that AZT and PSS are released gradually from the IBPD. The combined release of AZT and PSS may reach therapeutically effective levels for the prophylaxis of HIV and STIs. The flux of AZT and PSS across the pig vaginal tissue over time is shown in Fig. 4. A relatively constant increase in the rate of flux occurred over the initial 12 h and thereafter saturation was achieved up to 24 h. A mass balance was also

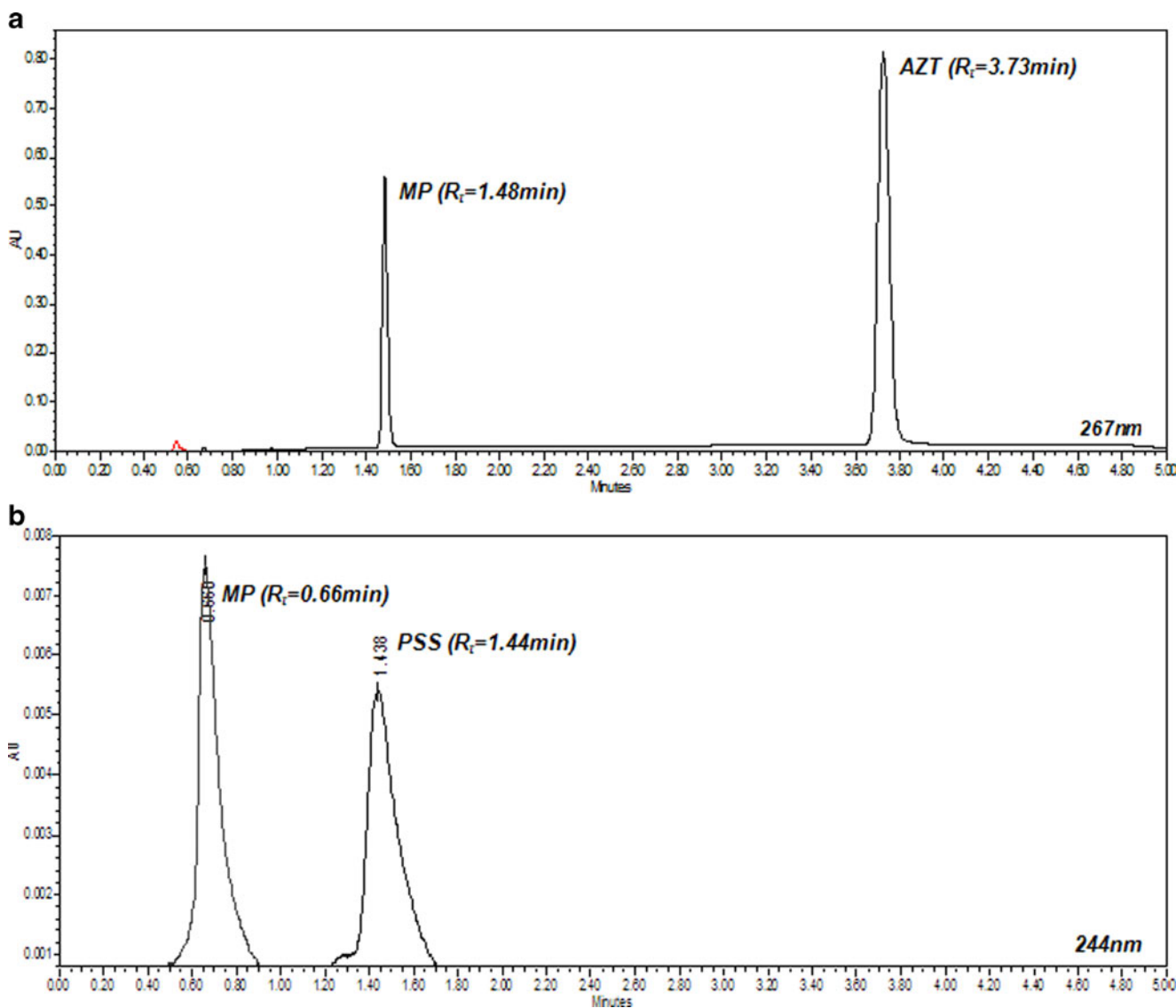


Fig. 1. UPLC chromatograms depicting the separation of **a)** AZT and MP (internal standard) and **b)** PSS and MP (internal standard) in SHVF (pH 4.5; 37°C)

achieved (Fig. 4). This suggests that the mechanism of passive drug transport across the pig vaginal tissue became saturated. The lower flux of PSS reflects its high degree of hydrophobicity coupled with the presence of strong intermolecular charges in the polymer (65–67). This may therefore have contributed to controlling the permeation of the drug across the vaginal tissue. Overall, it can therefore be proposed that the majority of drug was adsorbed onto the surface of the vaginal tissue.

Chemometric and Molecular Modeling of Drug Dissolution and Diffusion from the Intravaginal Bioadhesive Polymeric Device

Postulation of Dissolution Dynamics and Subsequent Effect on Drug Release

Chemometric and computational analysis conducted in our laboratories revealed that polymer–polymer and poly-

mer–drug ratios, as well as the ratio between the coating polymers and components of the dissolution medium contributed substantially to drug dissolution kinetics obtained. Figure 5 depicts a step-wise model of the IBPD undergoing dissolution.

Regarding the physicochemical associations of the polymers, AZT and PSS, all components were homogenous and produced a characteristic even distribution within the IBPD matrix. The hydrophilic and hydrophobic areas of certain polymeric components within the matrix and their association provided the flexible hydration sites. The hydrophilic sites were located within the outer regions of the matrix and the hydrophobic sites were confined to fewer interactive regions at the center of the IBPD matrix. AZT was confined near hydrophilic regions of the matrix while PSS consolidated the inner core as well as areas associated with other hydrophobic polymeric interactions such as PLGA and EC. This segregated hydrophile–hydrophobe clusters within the IBPD matrix was primarily responsible for modulating the diffusion

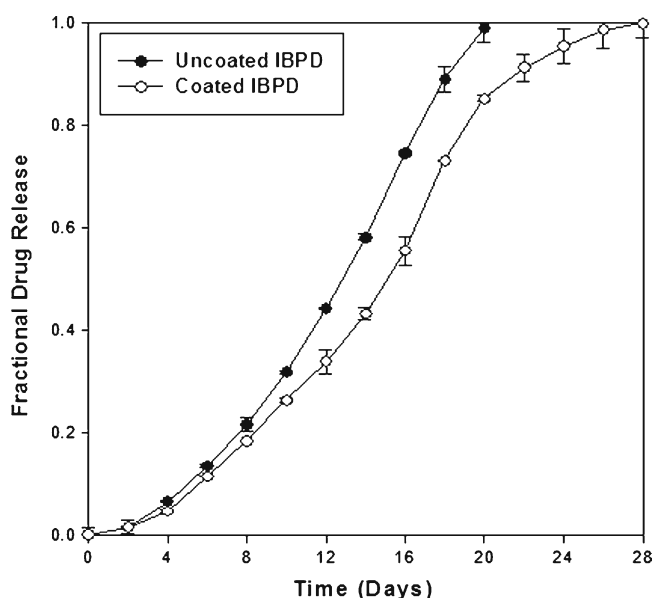


Fig. 2. A typical profile showing the effect of coating on the model hydrophilic drug AZT from an uncoated IBPD and a shellac/APE-PAA-coated IBPD in SHVF (pH 4.5; 37°C; $N=3$; $SD<0.18$ in all cases)

path of drug molecules through the matrix and subsequently controlling drug release. The chemometric and molecular modeling revealed that, remarkably, the rate of transport for the hydrophilic drug AZT compared to the hydrophobic PSS was found to be in a ratio of 3:2 indicating that AZT diffused at a rate that was 1.5 times faster than PSS. This explains the longer controlled release effect obtained when PSS was incorporated into the IBPD device. Through chemometric modeling, it was also ascertained that the difference in molecular mass between AZT and PSS was not solely responsible for this behavior and that the high degree of charge density in PSS, the ionic interactions between the

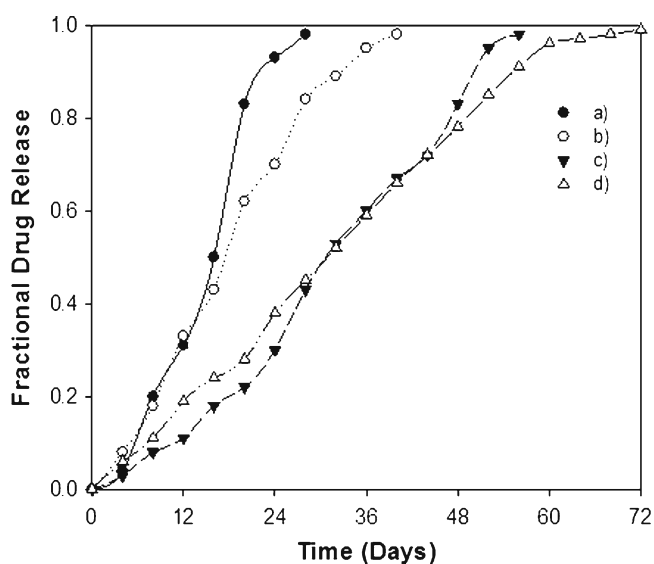


Fig. 3. Drug release profiles of coated IBPDs showing (a) AZT (AZT-loaded IBPD), (b) AZT (AZT/PSS-loaded IBPD), (c) PSS (AZT/PSS-loaded IBPD) and (d) PSS (PSS-loaded IBPD), in simulated vagina fluid (pH 4.5; 37°C; $N=3$; $SD<0.38$ in all cases)

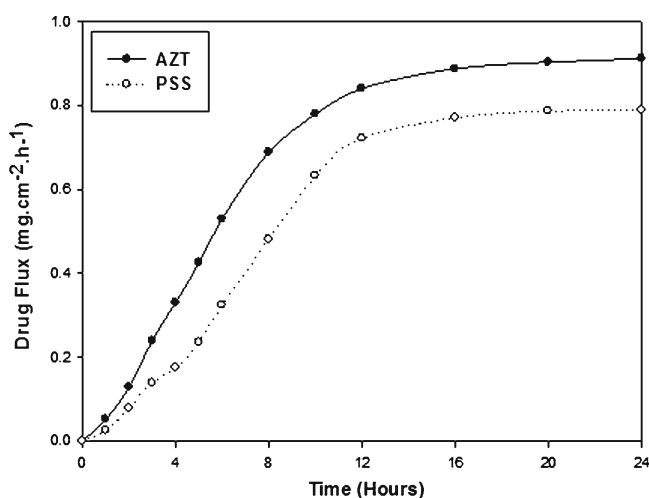


Fig. 4. Profiles showing the flux of AZT and PSS across pig vaginal tissue over a period of 24 h ($N=3$, $SD<0.23$ in all cases)

cationic PSS and the polymer constituents as well as the high osmotic coefficient and radius of gyration of PSS, were the primary contributing factors. Changes in vaginal fluid flow rate under normal condition, during sex, and/or menstruation and the presence of any resultant shear do not pose a major factor to interfere with the functionality of the IBPD due to the isolated site of application of the device.

Diffusion Kinetics Depicting the Drug Flux Mechanism During Ex Vivo Studies

The presence of excess SHVF led to complete dissolution of the caplet in the donor compartment of the Franz diffusion cell apparatus during the *ex vivo* vaginal tissue permeation studies weakening the interactions and physico-chemical associations. It was observed that approximately 21% of AZT and 14% of PSS permeated across the pig vaginal tissue in 24 h. The actual transport of the drugs (considering that 16% of both drugs, i.e., 200 mg each in a 1,200 mg IBPD matrix) from the donor compartment to the receptor compartment was 1.662 and 1.180 mg for AZT and PSS, respectively. This indicated that only 3.46% of AZT and 2.46% of PSS permeated through the pig vaginal tissue from the donor compartment to the receptor compartment of the Franz diffusion cells. Thus, the total drug transport across the vaginal tissue was computed as 5.92% with equilibrium achieved after 24 h. A chemometric model depicting the step-wise process of generating diffusion/transport channels perpendicularly to a polymer-strand localized in the IBPD is depicted in Fig. 6.

With regards to the diffusion kinetics of the IBPD device, the pH of the SHVF had a contributory effect on the transport of drug across the pig vaginal tissue. An osmotic gradient-mediated transport across the vaginal tissue based on the higher concentration of drugs, ions, and other molecular entities in the 2-mL donor compartment of the Franz diffusion cells. The permeation of drug was also inversely proportional to the molecular mass and almost all components, i.e., ions, drugs, polymeric strands, protein, salts, and acids as well as urea from the donor cell permeated though in varying concentrations. The considerable energy

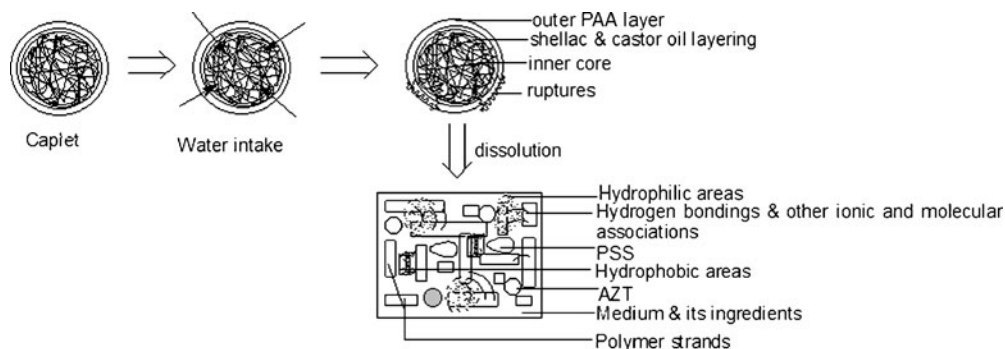


Fig. 5. Molecular model mechanistically depicting the IBPD dissolution process with lesser H-bond formation due to the excessive of SHVF providing more freedom for polymeric strands to disentangle

paradigms were governed by the solvation of the dissolution medium and osmotic flux. The qualitative status of energy paradigms and energy–time relationships for the IBPD matrix is as shown in Fig. 7a–c. A simple energy status is depicted as a qualitative energy–time relationship for the IBPD matrix as clearly portrayed in Fig. 7a–c.

Micro-environmental pH Variation Analysis Within the SHVF

It was generally observed that the superficial SHVF immediately adjacent to the immersed IBPD exhibited higher pH values than the SHVF immediately surrounding the device. The initial pH, measured as close as possible to the device, upon insertion of the IBPD into the titration system (MPT-2) was 4.5 ± 0.01 ($N=3$). The pH electrode was inserted using a Narashige micro-manipulator and was submerged towards the IBPD by careful hydraulic micro-movements to avoid creating any unnecessary turbulent hydrodynamic flow. A slight drop in pH was routinely recorded as the electrode passed in proximity to the IBPD with a slightly more acid pH than the entire SHVF ($\text{pH } 4.48 \pm 0.02$) around a superficial surface diameter of 5 mm. The pH, measured away from the superficial layer was 4.58 ± 0.03 ($N=3$). The relatively higher pH at the superficial layer may have been due to the extruding OH^- ions from mPA 6,10, EC, PAA, or PVA. The relatively lower pH observed at the IBPD proximity (micro-environmental pH) could most certainly have been due to the breakdown of PLGA into lactic and glycolic acids. This biphasic response in pH was observed over an experimental

period of 30 days. A profile depicting this sequence is shown in Fig. 8.

Attempts were made to perturb the inherent pH of the SHVF by adding incremental volumes of SHSF (52) ($\text{pH } 7.0$; 37°C) (Table I) (a significantly greater volume than would be produced on degradation of the PLGA-based IBPD in the SHVF) to simulate the presence of semen during/after sexual intercourse. After the addition of SHSF, the pH recorded within the SHVF was 4.58 ± 0.02 ($N=3$) and not significantly different from the resting pH of 4.50 ($P < 0.01$). Upon further addition of SHSF into the MPT-2, the inherent pH was reduced to 4.52 ± 0.03 ($N=3$) indicating that the SHVF was able to maintain its internal pH close to a value of 4.50 in the presence of a more alkaline medium (e.g., seminal fluid). Overall the results portrayed the potential of the IBPD to control and buffer the pH range of 3.5–5.5 in the SHVF by the virtue of the degradation of PLGA to lactic and glycolic acids. This pH range is the same as that produced by *Lactobacilli* species (68) which plays a vital role in keeping the vagina healthy. It also covers the average pH range of a normal healthy human vagina which is 4–5 (69–71) indicating the suitability of the IBPD for the intended purpose.

Thermal Analysis of the Composite Intravaginal Bioadhesive Polymeric Device

The thermal stability of the constituent polymers as well as the composite unhydrated IBPD was investigated by TMDSC at a temperature range from -35°C to 230°C . The polymers displayed multi-transitional thermal behaviors with multiple glass transition temperature (T_g), melting temper-

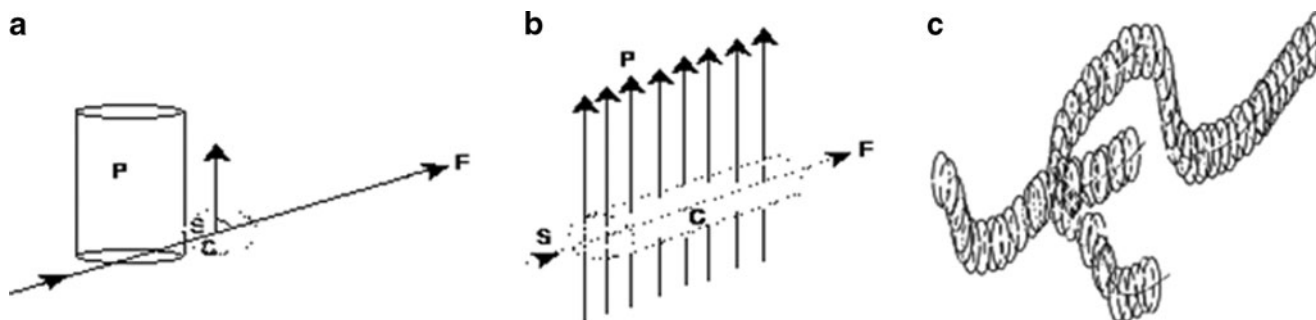


Fig. 6. Chemometric model depicting the development of a diffusion channel with **a**) a single polymer strand P , situated perpendicularly to a forming pore C , **b**) a group of strands also denoted collectively as P giving rise to the channel C which is formed perpendicular to the polymer strand backbone with F = the direction of flow from the starting point S to form a networked 3D channel and **c**) a polymeric strand with the generated diffusion channel

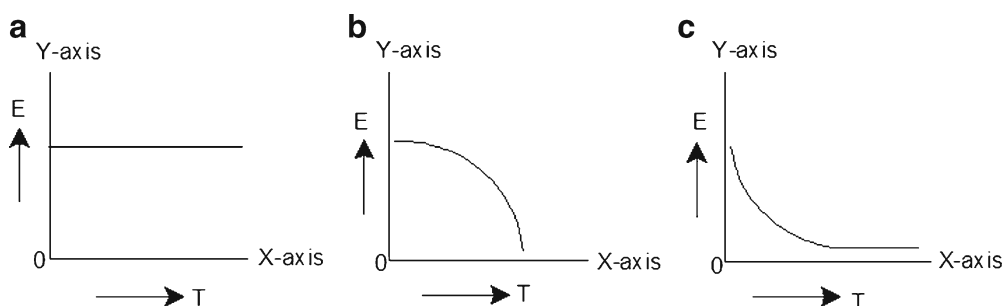


Fig. 7. Qualitative models of energy paradigms and energy–time relationships for the IBPD matrix with **a)** stable energy status as a solid matrix, **b)** energy change following dissolution, and **c)** energy transaction and changes for the drug permeation across the pig vaginal tissue with the static energy status at equilibrium without flux also shown

ature (T_m), and crystallization temperature (T_c) values (Table IV) that were attributed to the existence of reversing and non-reversing endothermic signals arising from the transient melting of molecules within each polymer.

Characterization of the Native Unhydrated Polymer Constituents of the IBPD

Ethylcellulose and Modified Polyamide 6,10

EC was characterized by a T_g at 100°C and an exothermic T_c at 130°C (Table IV). The T_m of EC occurred at 170°C which was relatively high compared to the other polymers. This revealed the superior thermodynamic stability of the polysaccharide subunits of EC. The m PA 6,10 had a distinct T_g at 163°C and two endothermic T_m values at 65°C and 140°C. In addition, two exothermic T_c peaks of m PA 6,10 were observed at 120°C and 200°C that followed the melting phases (Table IV). This suggested partial decomposition of m PA 6,10 that may be related to mass loss and the fact that the aliphatic polyamides inherently have a high heat of fusion and low entropy of fusion dependent on the collective dissociation energy of intramolecular H-bonds before any macroscopic dimensional changes can be realized (72,73).

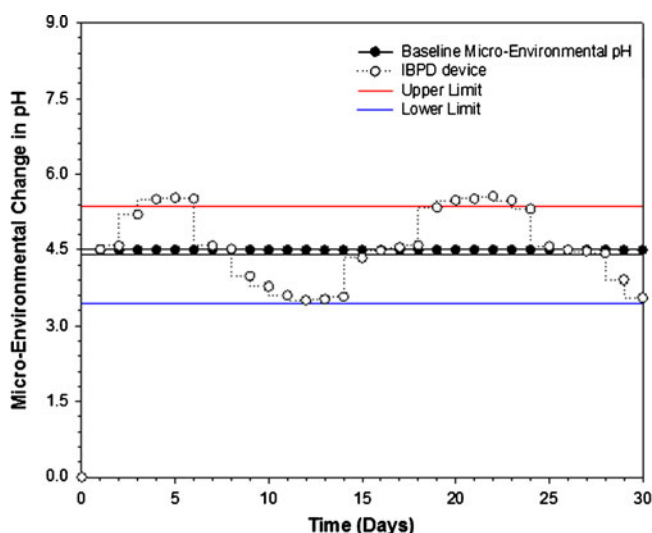


Fig. 8. Micro-environmental pH variation in the simulated vaginal fluid containing the IBPD ($N=3$)

Poly(lactic-co-glycolic Acid), Polyvinyl Alcohol, and Poly(acrylic Acid)

PLGA was characterized by two T_g values (Table IV). The first T_g peak appeared during the initial heating scan in which an enthalpy of relaxation peak superimposed the T_g between 45°C and 55°C. The second T_g value at 210°C was also noted as PLGA is a quench cooled amorphous material (74). As heating proceeded, the T_g and the temperature at the apex of the overheating peak shifted to higher temperatures ($T_g=210°C$; $T_m=220°C$; Table IV) due to the formation of a percolated network structure resulting from the quench cooling properties of PLGA. Thermograms for PVA revealed two T_g values at 22°C and 115°C and two endothermic T_m peaks at 30°C and 180°C (Table IV) due to the thermal decomposition of the ordered PVA elements. Thermodynamic analysis of PVA isotherms and crystallite growth rates has shown that crystallization of PVA (163°C; 215°C) is one dimensional (75). Thus, due to the absence of water or other swelling agents, kinetic hindrances predominated as a

Table IV. Critical Thermal Events Evidenced by Diverse Temperature Inflection Peaks for the Polymer Constituents of the Intravaginal Bioadhesive Polymeric Device

Sample analyzed	Critical temperature transition points (°C)		
	T_g	T_c	T_m
m PA 6,10	163	120; 200	65; 140
PLGA	45–55; 210	230	22; 220
APE-PAA	90	60	30; 130–170
PVA	22; 115	163; 215	30; 180
EC	100	130	170
Hydrated polymer blend	70; 160	210	22; 163; 200
Unhydrated polymer blend	170	220	200
Hydrated IBPD	83; 163	160	–10; 38; 85
Unhydrated IBPD	150	140; 220	222

T_g glass transition temperature, T_c crystallization temperature, T_m melting temperature

m PA 6,10 modified polyamide 6,10

PLGA poly(lactic-co-glycolic acid)

APE-PAA allyl penta erythritol-crosslinked polyacrylic acid

PVA polyvinyl alcohol

EC ethylcellulose

IBPD intravaginal bioadhesive polymeric device

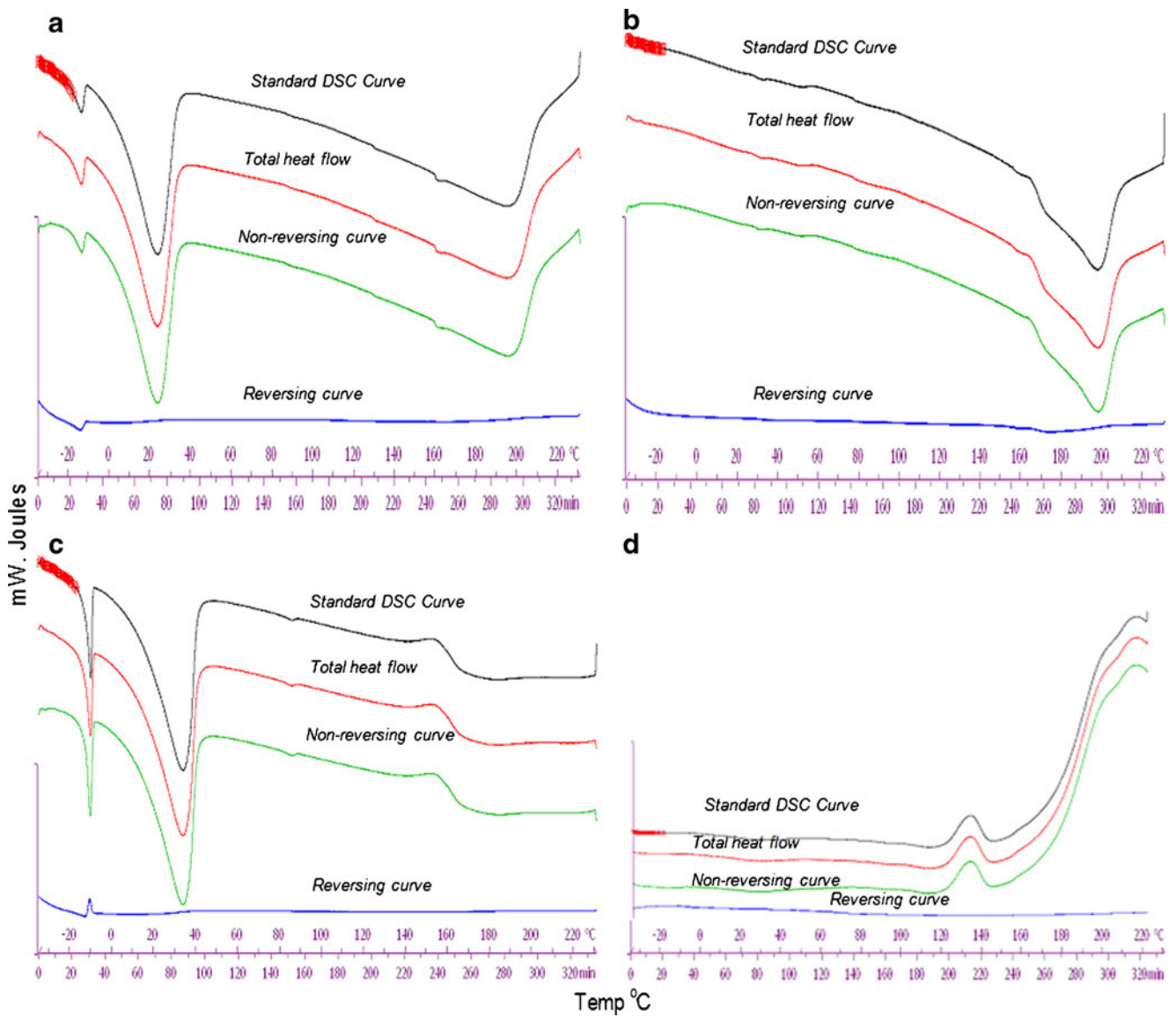


Fig. 9. TMDSC thermograms for a) the hydrated physical polymer blend, b) the unhydrated physical polymer blend, c) the hydrated IBPD, and d) the unhydrated IBPD

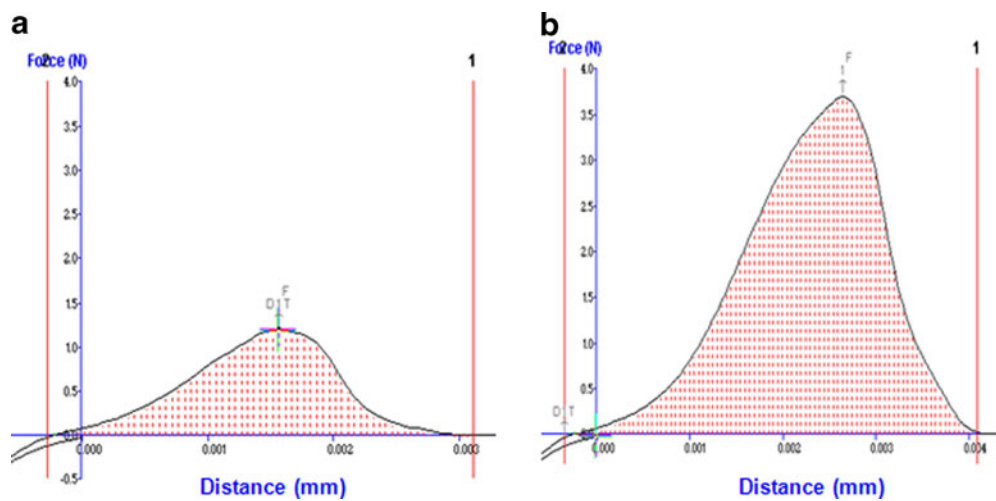


Fig. 10. Typical force–distance textural profiles used for computing the peak adhesion force and work of adhesion for a) uncoated devices and b) PAA-coated devices on freshly excised pig vaginal tissue

result of interactions between the OH groups of PVA. The salient thermal events for PAA are shown in Table IV. The broad endothermic peak (130–170°C) resulted from conformational changes in the macromolecules of PAA related to the magnitude of crosslinking interactions between the proton-donating pendent COOH⁻ groups and polar OH⁻ groups of PAA during synthesis (76). The presence of COOH⁻ groups favored the bioadhesiveness of PAA to the pig vaginal tissue when used as a coating agent for the IBPD device.

Characterization of the Unhydrated IBPD

Thermal analysis of the IBPD revealed a T_g at 150°C, two T_c peaks at 140°C and 220°C and a T_m peak at 220°C (Table IV). The presence of transient T_m peaks in the total TMDSC signals for the IBPD indicated that the polymers were dispersed within the device matrix. In addition, diminutive exothermic events were observed at the corresponding T_c ranges for the constituent polymers indicating a high degree of crystallinity within the device matrix structure. The deconvolution of the total TMDSC signals for the IBPD in terms of reversing and non-reversing events reflected the average of the equivalent signals for each polymer. However, for the IBPD the T_m appeared to be predominantly reversing due to the concurrent re-crystallization and melting phenomena that offset one another. This indicated that solid–solid phase transitions may have occurred within the IBPD due to polymeric compression, and subsequently contributed to the prolongation and control of drug from the device. Thus, the thermodynamic stability of polymers/polymer blends may affect the drug release process and can therefore be used to predict the drug release behavior based on unequivocally defined thermodynamic events.

Characterization of Unhydrated and Hydrated Physical Polymer Blends as well as Hydrated IBPD

TMDSC analysis was also performed on hydrated and unhydrated physical blends of the constituent polymers of the IBPD as well as the hydrated IBPD in order to determine the effect of compression on the polymer blend. Thermograms obtained on the hydrated and unhydrated physical polymer blends as well as the hydrated and unhydrated IBPD are depicted in Fig. 9 and Table IV. Overall, there was a distinct similarity between thermal events of the hydrated physical polymer blend and the hydrated IBPD (Fig. 9a and c). Thermograms presented with regions associated with very low temperatures (–10°C and –15°C) for the hydrated samples of the physical polymer blend and the IBPD while dehydration was complete at 200°C (Fig. 9a and c). However, the thermal behavior for the unhydrated physical polymer blend was markedly different from that of the unhydrated IBPD (Fig. 9b and d). This was attributed primarily to the effect of polymer compression on the physical polymer blend to produce the device.

For the hydrated physical polymer blend (Fig. 9a), the onset of the low-temperature endothermic T_m peaks (–15°C and 22°C) was attributed to the high moisture content in the physical polymer blend while the apparent T_m peaks (163°C and 200°C) resulted from the loss of residual water as heating

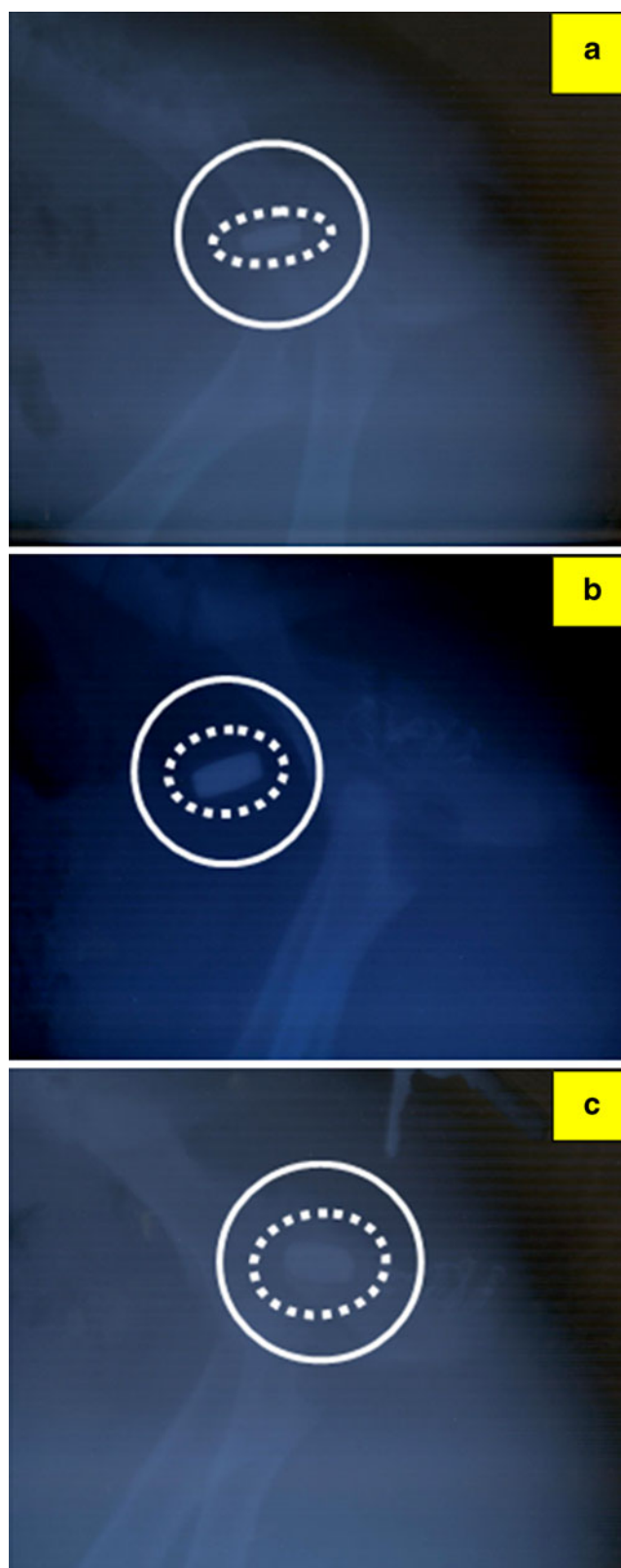


Fig. 11. X-ray images depicting the presence of the coated intra-vaginal bioadhesive polymeric device at **a)** day 1, **b)** day 14, and **c)** day 30 after insertion into the posterior fornix of the pig vagina

proceeded. The T_m endotherms were distinctly separated from the total heat flow in the non-reversing signal. Contrary to the hydrated physical polymer blend, the unhydrated polymer blend showed fewer thermal events (Fig. 9b). A single T_g at 170°C and a T_m peak at 200°C were observed (Fig. 9b). Furthermore, the T_g and T_m peaks that appeared for the hydrated physical polymer blend prior to 170°C, were absent in the unhydrated polymer blend (Fig. 9b). This may be associated with a baseline transition at $\pm 170^\circ\text{C}$ in the reversing heat flow signal. Overall, the hydrated physical polymer blend presented with lower T_m peaks (22°C and 163°C). These observations were consistent with previous results reported by Frushour (77) where, upon hydrating a physical polymer blend, the T_m peak was reduced well below the onset temperature.

Ex Vivo Bioadhesivity Analysis of the Intravaginal Bioadhesive Polymeric Device

The devices that were produced were strongly bioadhesive. Textural profile analysis indicated that the uncoated devices had the lowest bioadhesivity (PAF=1.1976 \pm 0.150 N; AUC_{FD}=0.0019 \pm 0.0001 J) compared with the PAA-coated devices (PAF=3.699 \pm 0.0464 N; AUC_{FD}=0.0098 \pm 0.0004 J; Fig. 10a and b). This indicates the superiority of APE-PAA as a bioadhesive coating as may be attributed to its hydrophilicity, H-bonding capacity, the high molecular mass, and the surface tension properties of the polymer. Polyacrylic controlled the extent of interpenetration between the polymer and the vaginal mucosal/epithelial surface. The high hydrophilicity of APE-PAA enabled the formation of strong bioadhesive bonds due to the high water content within the mucosal layer of the pig vaginal tissue. The presence of OH⁻ and COOH⁻ groups in APE-PAA may have favored the formation of H-bonds between the entangled APE-PAA chains and the pig vaginal tissue that ultimately resulted in bioadhesion. In addition, the desirable surface tension of PAA facilitated spreading over the epithelial surface of the vaginal mucosal layer thereby enhancing bioadhesion.

Retention of the Intravaginal Bioadhesive Polymeric Device Within the Pig Vagina

Analysis of X-ray images (Fig. 11) revealed that the coated devices were maintained in the posterior fornix of the pig vagina for the experimental period up to 30 days. The devices underwent swelling and gradually eroded over time as shown in Fig. 11a, b, and c which is in accordance with the stipulated design in which the formulation is expected to initially swell in order to facilitate bioadhesion and thereafter gradually erode and release the drug over the vaginal tissue for the required clinical preventative effect.

CONCLUSIONS

Robust polymeric devices were produced that confirmed the ability of the polymer blend selected ($_m\text{PA}$ 6,10, PLGA, PVA, PAA, and EC) to control the release of the model drugs AZT and PSS over a period of 72 days. The thermodynamic stability of the native polymers and device was substantiated by TMDSC thermograms. *Ex vivo* bioadhesion and permeation studies revealed that the APE-PAA-coated devices

were desirably bioadhesive and a relatively substantial fraction of the drug load was confined within the vaginal tissue. The produced IBPDs showed the potential of maintaining the acidic micro-environmental pH of the SHVF upon degrading which is a desirable feature in the vagina. The chemometric and molecular structural modeling approach qualitatively supported the deduction of the IBPD rate of dissolution and has shown that the drug release rate was dependent on the stoichiometric parameters between the polymers, drugs, and the SHVF. Furthermore, it was mechanistically deduced that the permeation of drug across the pig vaginal tissue during *ex vivo* studies was based on an osmotic gradient and depended on the degree of ionization as well as the size and molecular mass of the drug molecules. Thus, the developed IBPD may be suitable for use as a localized intravaginal drug delivery system for the potential treatment and prevention of HIV infection and STIs.

ACKNOWLEDGMENTS

This research is supported by the Norwegian Agency for Development Co-operation (NORAD)-NORWAY, and by grants from the National Research Foundation (NRF) of South Africa and the Faculty Research Committee, University of Witwatersrand, Johannesburg, South Africa. St. John's University of Tanzania is sincerely acknowledged.

Ethical Approval Ethics clearance for this study was obtained from the Animal Ethics Committee of the University of the Witwatersrand (Ethics clearance no. 2007/25/05).

REFERENCES

- Hussain A, Ahsan F. The vagina as a route for systemic drug delivery. *J Control Release*. 2005;103(12):301–13.
- Benkop-Schnurch A, Hornof M. Intravaginal drug delivery systems: design, challenges and solutions. *Am J Drug Deliv*. 2003;1(4):241–54.
- Iyer V, Bendgude N, Poddar SS. Vaginal drug delivery. *Express Pharma*. 2008. <http://www.expresspharmaonline.com/20080715/research02.shtml>. Accessed 19 March 2009.
- Cohen MS, Black JR, Proctor RA, Sparling PF. Host defenses and the vaginal mucosa: a re-evaluation. *Scand J Urol Nephrol*. 1984;86:3–22.
- Carrington GL, Rohrer T, Jones E, Moore P. Sulfanilamide absorption via the rectum and vagina. *Surg Gynecol Obstet*. 1944;78:333–4.
- Goldberger MA, Walter RI, Lapid LS. Absorption of penicillin from the vagina. *Am J Obstet Gynecol*. 1947;53:529–31.
- Mishell DR, Lumkin M, Stone S. Inhibition of ovulation with cyclic use progesterone-impregnated devices. *Am J Obstet Gynecol*. 1972;13:927–32.
- Fried ND, Tredway DR, Mishell DR. Termination of early pregnancy with prostaglandin E₂ vaginal suppositories. *Contraception*. 1973;8:255–63.
- Kirton KT, Roseman TJ, Forber AD. Evaluation of progesterone-containing silicone vaginal devices in rhesus monkeys. *Contraception*. 1973;8:561–8.
- Johansson EDB, Luukkainen T, Vartiainen E, Victor A. The effect of progestin R 2323 released from vaginal rings on ovarian function. *Contraception*. 1975;12:299–307.
- Nuwayser ES, Williams DL. Development of delivery system for prostaglandins. *Adv Exp Med Biol*. 1974;47:45–164.
- Verman K, Garg S. The scope and potential of vaginal drug delivery. *Pharm Sci & Technol Today*. 2000;3(10):359–64.

13. Valenta C, Constantia E, Kast CE, Harich I, Bernkop-Schnürch A. Development and *in vitro* evaluation of a bioadhesive vaginal delivery system for progesterone. *J Control Release*. 2001;77(3):323–32.
14. Yoo W, Dharmala K, Lee C. The physico-dynamic properties of bioadhesive polymeric films developed as female controlled drug delivery system. *Int J Pharm*. 2006;309(1–2):139–45.
15. Bonferoni MC, Sandri G, Rossi S, Ferrari F, Gibin S, Caramella C. Chitosan citrate as multifunctional polymer for vaginal delivery: evaluation of penetration enhancement and peptidase inhibition properties. *Eur J Pharm Sci*. 2007;33(2):166–76.
16. Wang L, Tang X. A novel ketoconazole bioadhesive effervescent tablet for vaginal delivery: design, *in vitro* and '*in vivo*' evaluation. *Int J Pharm*. 2008;350(1–2):181–7.
17. Valenta C. Bioadhesive polymers: strategies, achievements and future challenge. *Adv Drug Deliv Rev*. 2005;57(11):1692–712.
18. das Neves J, Bahia MF. Gels as vaginal drug delivery systems. *Int J Pharm*. 2006;318(1–2):1–14.
19. Ndesendo VMK, Pillay V, Choonara YE, Buchmann E, Bayever DN, Meyer LCR. Current intravaginal drug delivery approaches employed for the prophylaxis of HIV/AIDS and prevention of sexually transmitted infections. *AAPS PharmSciTech*. 2008;9(2):505–20.
20. Fauci AS. International Trial Of Two Microbicides Begins. *Science Daily*. 2005. <http://www.sciencedaily.com/releases/2005/02/050213135251.htm>. (accessed May 22, 2009).
21. Parija S, Nayak SK, Verma SK, Tripathy SS. Studies on physico-mechanical properties and thermal characteristics of polypropylene/layered silicate nanocomposites. *Polymer Compos*. 2004;25(6):646–52.
22. Liu TX, Liu ZH, Ma KX, Shen L, Zeng KY, He CB. Morphology, thermal and mechanical behavior of polyamide 6/layered-silicate nanocomposites. *Comp Sci Tech*. 2003;63(3–4):331–7.
23. Ribeiro M, Grolier JPE. Temperature modulated DSC for the investigation of polymer materials: a brief account of recent studies. *J Therm Anal Calorim*. 1999;57(1):253–63.
24. Pijpers TFJ, Mathot VBF, Goderis B *et al*. High-speed calorimetry for the study of the kinetics of (De) vitrification, crystallization, and melting of macromolecules. *Macromol*. 2000;35(9):3601–13.
25. Sudhakar Y, Kuotsu K, Bandyopadhyay AK. Buccal bioadhesive drug delivery—a promising option for orally less efficient drugs. *J Control Release*. 2006;114:15–40.
26. Avdeef A, Artursson Sibylle Neuhoff S *et al*. Caco-2 permeability of weakly basic drugs predicted with the Double-Sink PAMPA pK_a^{flux} method. *Eur J Pharm Sci*. 2005;24(43):333–49.
27. Van Itallie CM, Anderson JM. The Molecular Physiology of Tight Junction Pores Physiology. 2004;19:331–8.
28. Garg S, Verman K, Anderson RA, Zaneveld LJ. Rapidly disintegrating novel bioadhesive vaginal tablets of polystyrene sulfonate (PSS), a potential microbicide formulation, International Conference of AIDS, July 11–16 2004; Abstract No. TuPeB4656.
29. Chu H, Yeo Y, Chuang KS. Entry in emulsion polymerization using a mixture of sodium polystyrene sulfonate and sodium dodecyl sulfate as the surfactant. *Polymer*. 2007;48(8):2298–305.
30. Anderson RA, Feathergill X, Diao M, Cooper R, Kirkpatrick P, Spear DP *et al*. Evaluation of poly (styrene-4-sulfonate) as a preventive agent for conception and sexually transmitted diseases. *J Androl*. 2000;121(6):862–75.
31. Simoes JA, Citron DM, Aroucheva A, Anderson RA, Chany CJ, Waller DP *et al*. Two novel vaginal microbicides (polystyrene sulfonate and cellulose sulfate) inhibit *Gardenerella vaginalis* and anaerobes commonly associated with bacterial vaginosis. *Antimicrob Agents Chemother*. 2002;46(8):2692–5.
32. Bourne N, Zaneveld LJD, Ward JA, Ireland JP, Stanberry LR. Poly (sodium 4-sulfonate): evaluation of a topical microbicide gel against herpes simplex virus type 2 and *Chlamydia trachomatis* infection in mice. *Clin Microbiol Infect*. 2003;9:816–22.
33. D'Cruz OJ, Uckun FM. Clinical development of microbicides for the prevention of HIV infection. *Curr Pharm Des*. 2004;10(3):315–35.
34. Keller MJ, Tuyama A, Carlucci MJ, Herold BC. Topical microbicides for the prevention of genital herpes infection. *J Antimicrob Chemother*. 2005;55:420–3.
35. Bonacucina G, Cespi M, Misici-Falzi M, Palmieri GF. Rheological, adhesive and release characterisation of semisolid carbopol/tetraglycol systems. *Int J Pharm*. 2006;307(2):129–40.
36. Ndesendo VMK, Pillay V, Choonara YE, Khan RA, Meyer L, Buchmann E *et al*. *In vitro* and *ex vivo* bioadhesivity analysis of polymeric intravaginal caplets using biocompatibility and computational structural modeling. *Int J Pharm*. 2009;370(1–2): 151–9.
37. Pond WG, Haupt KA. Reproductive physiology. The Biology of the Pig. New York: Cornell University Press; 1988. p. 129–80.
38. D'Cruz OJ, Erbeck D, Uckun FM. A study of the potential of the pig as a model for the vaginal irritancy of benzalkonium chloride in comparison to the nonirritant microbicide PHI-443 and the spermicide vanadocene dithiocarbamate. *Toxicol Pathol*. 2005;33:465–76.
39. Wang Z, Li X, Su D, Li Y, Wu L, Wang Y *et al*. Residue depletion of Imidocarb in swine tissue. *J Agric Food Chem*. 2009;57:2324–8.
40. Bailey ML, Swett JE. Radiopaque compositions, articles and methods of making and using same. USPTO Patent Application 20070270691. 2007. <http://www.freshpatents.com/Radiopaque-compositions-articles-and-methods-of-making-and-using-same-20071122ptan20070270691.php>. Accessed 05 April 2009.
41. Park JH, Ye M, Park K. Biodegradable polymers for micro-encapsulation of drugs. *Molecules*. 2005;10(1):146–61.
42. Yasukawa T, Ogura Y, Kimura H *et al*. Drug delivery from ocular implants. *Expert Opin Drug Deliv*. 2006;3(1):261–73.
43. Kulkarni A, Reiche J, Lendlein A. Hydrolytic degradation of poly(*rac*-lactide) and poly[(*rac*-lactide)-*co*-glycolide] at the air-water interface. *Surf Interface Anal*. 2007;39(9):740–6.
44. Kolawole OA, Pillay V, Choonara YE. Novel modified polyamide 6, 10 variants synthesized by modified interfacial polymerization for application as a rate-modulated monolithic drug delivery System. *J Bioact Comp Polym*. 2007;22:281–313.
45. Iseki T, Takahashi M, Hattori H, Hatakeyama T, Hatakeyama H. Viscoelastic properties of xanthan gum hydrogels annealed in the sol state. *Food Hydrocoll*. 2001;15(4–6):326.
46. Gimeno E, Moraru CI, Kokini JL. Effects of xanthan gum and CMC on the structure and texture of corn flour pellets expanded by microwave heating. *Cereal Chem*. 2003;81(1):100–7.
47. Verhoeven E, Vervaet C, Remon JP. Xanthan gum to tailor drug release of sustained-release ethylcellulose mini-matrices prepared via hot-melt extrusion: *in vitro* and *in vivo* evaluation. *Eur J Pharm Biopharm*. 2006;63(3):320–30.
48. Umamaheshwari RB, Ramteke S, Jain NK. Anti-*Helicobacter pylori* effect of bioadhesive nanoparticles bearing amoxicillin in experimental gerbils model. *AAPS PharmSciTech*. 2004;5:2.
49. Charde S, Mudgal M, Kumar L, Saha R. Development and evaluation of buccoadhesive controlled release tablets of lercanidipine. *AAPS PharmSciTech*. 2008;9(1):182–90.
50. Owen DH, Katz DF. A vaginal fluid stimulant. *Contraception*. 1999;59(2):91–5.
51. Giannola LI, De Caro V, Giandalia G, Siragusa MG, Tripodo, Florena AM *et al*. Release of naltrexone on bucal mucosa: permeation studies, histological aspects and matrix system design. *Eur J Pharm Biopharm*. 2007;67:425–33.
52. Owen DH, Katz DF. A review of the physical and chemical properties of human semen and the formulation of a semen simulant. *J Androl*. 2005;26:459–69.
53. Notari S, Bocedi A, Ippolito G, Narciso P *et al*. Simultaneous determination of 16 anti-HIV drugs in human plasma by high-performance liquid chromatography. *Journal Chromatogr B*. 2005;831(1–2):258–66.
54. Sinha VR, Kumria R. polymers for colon specific drug delivery. A comparative *in vitro* evaluation. *Acta Pharm*. 2003;53:41–7.
55. Singh MP, Lumpkin JA, Rosenblatt J. Effect of electrostatic interactions on polylysine release rates from collagen matrices and comparison with model predictions. *J Control Release*. 1995;35(2–3):165–79.
56. Vishalakshi B. The effect of the charge density and structure of the polymer on the dye-binding characteristics of some cationic polyelectrolytes. *J Polym Sci: Polym Chem*. 1995;33:365–71.
57. Jiang Y, Emau P, Cairns JS, Flanary L, Morton WR, McCarthy TD *et al*. SPL7013 gel as a topical microbicide for prevention of vaginal transmission of SHIV in macaques. *AIDS Res Hum Retroviruses*. 2005;21:207–13.

58. Bonifazi D, Enger O, Diederich F. Supramolecular [60]fullerene chemistry on surfaces. *Chem Soc Rev*. 2007;36:390–414.
59. Alvarez-Lorenzo C, Gomez-Amoza JL, Martinez-Pacheco R, Souto C. Microviscosity of hydroxypropylcellulose gel as a basis for prediction of drug diffusion rates. *Int J Pharm*. 1999;180:91–103.
60. Griffiths PC, Paul A, Khayat Z *et al.* Understanding the mechanism of action of poly(amidoamine)s as endosomolytic polymers: correlation of physicochemical and biological properties. *Biomacromol*. 2004;5(4):1422–7.
61. Le Cer RD, Picton L, Argillier JF, Muller G. Entrapment and release of sodium polystyrene sulfonate (SPS) from calcium alginate gel beads. *Eur Polym J*. 2004;40(12):2709–15.
62. Sen AK, Roy S, Juvekar VA. Effect of structure on solution and interfacial properties of sodium polystyrene sulfonate (NaPSS). (2007). *Polym Int*. 2007;56(2):167–74.
63. Thapa P, Stevens HNE, Baillie AJ. *In vitro* drug release studies from a novel lyophilized nasal dosage form. *Kathmandu University J Sci Tech*. 2009;5(1):71–86.
64. Viridén A, Wittgren B, Larsson A. Investigation of critical polymer properties for polymer release and swelling of HPMC matrix tablets. *Eur J Pharm Sci*. 2009;36(2–3):297–309.
65. Knudsen KD, Lauten RA, Kjøniksen A, Nyström B. Rheological and structural properties of aqueous solutions of a hydrophobically modified polyelectrolyte and its unmodified analogue. *Eur Polym J*. 2004;40(4):721–33.
66. Pu Q, Ng S, Mok V, Chen SB. Ion bridging effects on the electroviscosity of flexible polyelectrolytes. *J Phys Chem B*. 2004;108(37):14124–9.
67. Chu H, Yeo Y, Chuang KS. Entry in emulsion polymerization using a mixture of sodium polystyrene sulfonate and sodium dodecyl sulfate as the surfactant. *Polym*. 2007;48(8):2298–305.
68. Boskey, E. A., Jansen, M., Merski, I.K., Whaley, I.T., Moench, T. and Cone, R., BufferGel™ favors *in vitro* growth of *Lactobacilli* while inhibiting BV-associated organisms *Johns Hopkins University and ReProtect, Inc. Abstract A07*. 2000. <http://curezone.com/blogs/fm.asp?i=974816> [Accessed October 9, 2009].
69. Smith KPB. Estrogens and the urogenital tract. Studies on steroid hormone receptors and a clinical study on a new estradiol releasing vaginal ring. *Acta Obstet Gynecol Scand*. 1993;72:S1–26.
70. Ferris DG, Francis SL, Diman ED *et al.* Variability of vaginal pH determination by patients and clinicians. *J Am Board Fam Med*. 2006;19:368–73.
71. WebMD. Vaginal Wet Mount. *Women Health*. 2008. <http://women.webmd.com/vaginal-wet-mount> [Accessed September 9, 2009].
72. de Candia F, Maglio G, Palumbo R, Sirletti M. Synthesis and physical behavior of modified polyamide 6, 10-poly(butadiene-co-acrylonitrile) segmented block copolymers. *Colloid Polym Sci*. 1998;267(1):9–15.
73. Murthy NS. Hydrogen bonding, mobility, and structural transitions in aliphatic polyamides. *J Polym Sci B Polym Phys*. 2006;44(3):1763–82.
74. Rouse JJ, Mohamed F, van der Walle CF. Physical ageing and thermal analysis of PLGA microspheres encapsulating protein or DNA. *Int J Pharm*. 2007;339(1–2):112–20.
75. Peppas NA, Hansen PJ. Crystallization kinetics of poly(vinyl alcohol). *J Appl Polym Sci*. 2003;27(12):4787–97.
76. Sugama T, Kukacka LE, Carciello N. Nature of interfacial interaction mechanisms between polyacrylic acid macromolecules and oxide metal surfaces. *J Mater Sci*. 1984;19:4045–56.
77. Frushour BG. A new thermal analytical technique for acrylic polymers. *Polym Bulletin*. 2004;4(5):305–14.